PDGFD up-regulation due to reversible promoter demethylation contributes to gemcitabine resistance via STAT3 activation

Li Qin[1,$], Hao Liu[2], Jenny Beebe[1], Yangyang Hao[3], Zizheng Dong[5], Yunlong Liu[3], Zhimin He[2], Jing-Yuan Liu[4], Jian-Ting Zhang[1,5,*]

[1]Department of Pharmacology and Toxicology, Indiana University School of Medicine, Indianapolis, IN 46202

[2]Affiliated Cancer Hospital & Cancer Research Institute, Guangzhou Medical University, Guangzhou, 510095, Guangdong, China

[3]Department of Molecular and Medical Genetics, Indiana University School of Medicine, Indianapolis, IN 46202

[4]Department of Medicine, University of Toledo College of Medicine and Life Sciences, Toledo, OH 43614.

[5]Department of Cancer Biology, University of Toledo College of Medicine and Life Sciences, Toledo, OH 43614.

Running title: Reversible promoter demethylation and gemcitabine resistance

Conflict of interest statement: The authors declare no conflict of interests

[$]Current address: Institute of Hematology and Blood Diseases Hospital, Chinese Academy of Medical Sciences and Peking Union Medical College, Tianjin, China.

*To whom correspondence should be addressed. Department of Cancer Biology, University of Toledo College of Medicine and Life Sciences, 3000 Arlington Ave., MS1010, Toledo, OH 43614. Tel (419) 383-4100; Fax (419) 383-6228; Email jianting.zhang@utoledo.edu

ABSTRACT

Background and Purpose. Drug resistance is a major problem in cancer treatment with traditional or targeted therapeutics. Gemcitabine, a traditional chemotherapeutics, is approved for several human cancers and the first line treatment for locally advanced or metastatic pancreatic ductal adenocarcinoma (PDAC). However, gemcitabine resistance is frequently observed and a major problem in successful treatments of these cancers and the mechanism of gemcitabine resistance remains largely unknown. In this study, we aim to seek new and understand the molecule mechanisms of gemcitabine resistance in PDAC.

Experimental Approach. Using whole genome Reduced Representation Bisulfite Sequencing analysis, we investigated a gemcitabine resistant PDAC cell line M3K compared with its parental MiaPaCa-2 cells and the resistance revertant cell line Rev followed by detailed analyses of PDGFD in gemcitabine resistance using MTT survival assay, bisulfite sequencing, Western blot, siRNA knockdown and over-expression.

Key Results. We found that 65 genes had reversible methylation changes in their promoters in gemcitabine resistant PDAC cells. One of these genes, PDGFD, was further studied in detail for the reversible methylation change in its promoter and shown to reversibly up-regulate in expression, contribute to gemcitabine resistance in vitro and in vivo via activating STAT3 signaling in both autocrine and paracrine manners. Its expression also positively associates with poor outcome of PDAC patients.

Conclusion and Implications. Reversible epigenetic regulation may play an important role in gemcitabine resistance and targeting PDGFD signaling may alleviate gemcitabine resistance for PDAC treatment.

KEYWORDS

Drug resistance, epigenetic regulation, methylation, STAT3, gemcitabine, PDGFD, pancreatic ductal adenocarcinoma

ABBREVIATIONS

PDGFD, platelet-derived growth factor D; PDAC, pancreatic ductal adenocarcinoma; DNMT, DNA methyltransferase; RRBS, reduced representation bisulfite sequencing; STAT, signal transducer activator transcription

INTRODUCTION

Although appropriate combinations of chemotherapeutics have improved lives of cancer patients, drug resistance frequently occurs and severely hinders successful treatments of human cancers. Gemcitabine, a deoxycitidine analogue, has been approved for treating several human cancers including cancers of breast, lung, ovary, and pancreas and as the first-line chemotherapeutic drug for patients with locally advanced or metastatic pancreatic ductal adenocarcinoma (PDAC). However, gemcitabine resistance is a major problem and essentially all pancreatic cancer patients will develop and/or acquire gemcitabine resistance, contributing to the low (<8%) 5-year survival rate of PDAC patients.

Acquired gemcitabine resistance has been studied with a few mechanisms proposed including increased expression of nucleoside importer hENT1 and ribonucleotide reductase RRM1 in the gemcitabine metabolism pathway (Voutsadakis, 2011). Recently, it was found that PDAC cells may reversibly alter epigenetic regulation of gene expression to survive gemcitabine insult. In particular, 14-3-3σ gene is reversibly demethylated, resulting in up-regulation of its expression (Qin, Dong & Zhang, 2014) and contributes to the acquired gemcitabine resistance via the hippo-YAP pathway (Qin, Dong & Zhang, 2016). These findings raise a possible involvement of epigenetic regulation of gene expression in cellular response to gemcitabine and in gemcitabine resistance of PDAC cells.

To test this possibility and to understand the involvement of global epigenetic changes in cellular response to gemcitabine and its potential role in gemcitabine resistance, we performed comparative whole genome Reduced Representation Bisulfite Sequencing (RRBS) analysis and identified 65 genes with reversible promoter methylation change that associate with gemcitabine resistance. One of these genes, PDGFD was further studied and shown to contribute to both

acquired and intrinsic gemcitabine resistance by activating STAT3 signaling pathway in both autocrine and paracrine manners. These findings suggest that changes in epigenetic regulation may alter drug response of PDAC cells, which in turn may affect neighboring cells via paracrine effect.

MATERIALS AND METHODS

Materials. Metafectene Pro transfection reagent was obtained from Biontex. PDGFD siRNAs were purchased from Santa Cruz Biotechnology. CpGenome Universal DNA Modification kit was purchased from EMD Millipore. Antibodies against pSTAT3 (#9145), total STAT3 (#9139), Ki67 (#9027), and cleaved caspase-3 (#9661) were from Cell Signaling. Antibodies against PDGFD for Western blot and immunohistochemistry were from Sigma (SAB1401847) and Abcam (ab240960), respectively. PDGFD cDNA was from Thermo Scientific. RNeasy Mini kit and Qiagen Blood and Cell Culture DNA Kit were from Qiagen. The iScript^{TM} cDNA synthesis kit and the SYBR Green PCR master mix were from Bio-Rad and Applied Biosystems, respectively. Gemcitabine were from Besse Medical. The PDGFD siRNA (sc-39709) was from Santa Cruz and the shRNAs (ACGATGGTGTGGACACAAGGAAGTTCCTC and TGTCAACTGGAGGTCCTGCACATGCAATT) were from Origene (TG302563).

Reduced representation bisulfite sequencing (RRBS) and data analysis. RRBS was performed by BGI (Hong Kong, China). Briefly, genomic DNA was isolated from MiaPaCa-2, G3K, and Rev cells using Qiagen Blood and Cell Culture DNA Kit. For each cell line, three independent preparations were mixed in equal proportions before shipping to BGI for quality control testing and sequencing.

The raw read data were filtered to remove adapter sequence, contaminations and low quality reads before aligning to the genome using BGI SOAPaligner version 2.01 (Li et al., 2009).

Due to the strand specificity of DNA methylation, each bisulfite-converted read pair were aligned twice: (1) the observed cytosines on the forward read of the pair were converted in silico to thymines and mapped to the genome converted in the same way, and (2) the observed guanines on the reverse read of the pair were converted in silico to adenosines and mapped to the genome converted in the same way. To estimate methylation level and to exclude sequencing errors, only bases with quality >14 were considered. The level estimation is derived by dividing the number of converted cytosines in the region by the total number of bases covering CpG cytosines in that region. Differentially-methylated regions (DMR) were derived from windows with at least 5 CpG's and a 2-fold change in methylation level, and with Fisher's exact test $p<0.01$, as previously described (Li et al., 2010a).

Cell cultures and transfections. Human PDAC cell line MiaPaCa-2 and its derivative G3K and Rev were cultured in DMEM supplemented with 10% fetal bovine serum (FBS) and 2.5% horse serum. For G3K cells, 3 μM gemcitabine was added to maintain its resistance phenotype. Human PDAC cell line AsPC-1 was cultured in RPMI medium supplemented with 10% FBS. Human PDAC cell line Colo-357 and Colo-357R were cultured in DMEM supplemented with 10% FBS. For Colo-357R cells, 1 μM gemcitabine was used to maintain its resistance phenotype. The cell lines were authenticated by analysis of tandem repeat sequences on September 17, 2013.

For transient knockdown or overexpression, $1.5\text{-}3\times10^5$ cells/well were plated in six-well plates and cultured overnight in complete medium followed by transfection with 60-120 pmol siRNAs or 1-2 μg plasmid in serum-free Opti-MEM medium and using Metafectene Pro transfection reagent as previously described (Qin, Dong & Zhang, 2014). The stable clones were selected using 1 mg/ml G418 as previously described (Han, Xie, Chen & Zhang, 2006; Liu, Liu, Han & Zhang, 2006) and maintained in complete medium supplemented with 200 μg/ml G418.

Sample preparation and Western blot analysis. To prepare cell extract, cells were harvested, washed with PBS, and lysed in TNN-SDS buffer (50 mM Tris-HCl, pH 7.5, 150 mM NaCl, 0.5% Nonidet P-40, 50 mM NaF, 1 mM sodium orthovanadate, 1 mM dithiothreitol, 0.1% SDS, and 2 mM phenyl-methylsulfonyl fluoride) for 30 minutes at 4°C with constant agitation. The lysates were then sonicated briefly followed by centrifugation (16,000×*g* at 4°C) for 15 minutes. The supernatant was collected for protein concentration measurement using Bradford assay.

Membrane fractions were isolated as described previously (Yang, Chen & Zhang, 2002). Briefly, cells were washed with ice-cold PBS and resuspended in hypotonic lysis buffer (10 mM KCl, 1.5 mM $MgCl_2$, 10 mM Tris-HCl, pH 7.4, 2 mM PMSF) followed by homogenization and centrifugation at 4,000×*g* for 10 min at 4°C. The supernatant was collected and centrifuged again at 100,000×*g* for 1.5 hours to collect crude membrane fraction.

To prepare samples from conditioned media, cells were cultured in serum-free media for 24 hours and the media were centrifuged to remove cell debris followed by precipitation of proteins using trichloroacetic acid and centrifugation (14,000×*g*) at 4°C for 5 minutes. The pellet was washed by pre-chilled acetone and solubilized in SDS sample buffer.

Western blot analysis were performed as previously described (Qin, Dong & Zhang, 2014). Briefly, proteins were separated by SDS-PAGE and transferred to PVDF membranes followed by blocking in 5% nonfat milk and 0.1% Tween 20 and then incubation with primary antibodies. After extensive washing, immunoreactivity was detected using secondary antibody-conjugated horseradish peroxidase. Signals were captured using ECL and x-ray film.

Quantitative RT-PCR. Quantitative RT-PCR was performed as previously described (Dong et al., 2009; Liu et al., 2007). Briefly, total RNAs were extracted using RNeasy Mini Kit followed

by reverse-transcription using iScript^{TM} cDNA synthesis kit and quantitative PCR using the SYBR Green PCR master mix. The primer pairs used are shown in **supplemental Table S1**:

Survival assay. Survival assay was performed as previously described using MTT colorimetric or methylene blue-staining assays (Li et al., 2010b; Yang et al., 2007). Briefly, 2000-3000 cells/well were seeded in 96-well plates and cultured for 24 hrs followed by treatment with gemcitabine for 3 days. For MTT assay, MTT were added to cells to a final concentration of 0.5 mg/mL and incubated at 37°C for 4 hours followed by determination of OD570nm. For methylene blue assay, media was removed and cells were stained using 1% (w/v) methylene blue for 30 minutes. Excess dye was removed by aspiration and washing. The cell-retained dye was then released using a 1:1 mixture of 100% ethanol and 0.1 M HCl followed by determination of OD650 nm. The data were analyzed using GraphPad Prism to generate IC_{50}. Relative resistance factor (RRF) is calculated using $RRF=IC_{50(test)}/IC_{50(control)}$.

Sodium-bisulfite sequencing. Genomic DNAs were first modified by sodium bisulfite using the CpGenome universal DNA modification kit according to supplier's instructions. Ten-μg bisulfite-modified genomic DNAs were first amplified using primers 5′-TGAGTTTTTATAGGTTTAATTAGGAGGG-3′ and 5′-ACTCTCCCCAAACTTCCTACATACTA-3′ (for PDGFD gene) and subcloned into pGEM-T vectors (Promega). Four independent clones for each cell line were isolated and subjected to DNA sequencing.

Gemcitabine response of PDAC xenograft tumors. 1×10^6 stable MiaPaCa-2 cells transfected with vector (Vec) or over-expressing PDGFD (PD1) were injected subcutaneously in the flanks of 4-6 week old female nude mice. When tumor volume reached ~50 mm^3, the mice were randomized into three groups each (Vec and PD1) with five in each group followed by

treatments with PBS vehicle, 60 mg/kg or 120 mg/kg gemcitabine via IP injection twice a week for total 6 treatments. Tumor volume and body weight were measured every four days. On day 21, mice were euthanized and the tumor tissues were harvested, weighed, and subjected to hematoxylin and eosin (H&E) and immunohistochemistry staining of PDGFD, Ki67, and cleaved caspase 3 as previously described (Huang et al., 2016; Qi et al., 2016).

Overall survival analyses of PDAC patients. Kaplan Meier-plotter (KM plotter) (http://kmplot.com/analysis/) was used that can assess the association of many genes with patient survival of various cancers (Lanczky et al., 2016). The analyses of PDAC patients in the TCGA database were conducted with the cutoff at 60 months and with the hazard ratio (HR) at 95% confidence intervals and log rank $P<0.05$ considered significant.

Statistical analysis. Statistical analysis for all experiments was run using Prism. Results are presented as ±SD. IC50 values and real-time RT-PCR threshold cycles were calculated from 5 biological replicates which were each run in triplicate. Western blots were run on 5 different sample preps. All data were normalized to control for each run to reduce variation and the mean of the experimental groups was used for statistical analysis. Two-tailed T-test was used for comparing two means and ANOVA using the Tukey post hoc test for comparing a group of mean values with $p<0.05$ considered statistically significant.

RESULTS

Differentially methylated genomes in gemcitabine resistant G3K, its parental MiaPaCa-2 and the resistance-revertant Rev cells. To determine global changes in DNA methylation during acquisition of gemcitabine resistance, we performed Reduced Representation Bisulfite Sequencing (RRBS) analysis of isolated genomic DNAs from the parental MiaPaCa-2 cells, its gemcitabine-selected derivative clone G3K, and the partially resistance-revertant Rev cells (**Fig. 1A**). RRBS

yielded about 65~70 million clean reads for each cell line with mapped reads of >92%, uniquely mapped reads of >70%, and unique reads with enzyme cutting site of >97% **(Fig. 1B)**. Moreover, the RRBS targeted a reasonable proportion of genome of interest in all samples, with >70% of promoter and >83% of CG island (CGI) coverage, respectively (**Fig. 1C**). The individual CpG sites within CGIs and promoters were also examined, revealing good and consistent coverage at both 4X and 10X depths in all samples (**Fig. 1D**).

In total, 845 genes are differentially methylated between MiaPaCa-2 and G3K cells and 282 genes between G3K and Rev cells (**Fig. 1E**). These differentially methylated genes are shown in **Supplemental Tables S2, S3,** and **S4**. Because altered methylations in the promoter region most likely influence gene expression, we filtered these genes with differential methylation in the promoter region and with a 2-fold change cutoff, resulting in 159 genes with increased and 459 genes with decreased methylation in G3K compared with MiaPaca-2 cells **(Fig. 1E).** It also resulted in 104 genes with increased and 88 genes with decreased methylation in Rev compared with G3K cells. Of these genes, total 65 genes have reversible change in methylation status from MiaPaCa-2 to G3K and from G3K to Rev cells (**Table 1)**.

Expression of genes with reversible methylation change. Among these 65 genes, 10 were cherry picked for expression analysis using real-time RT-PCR. **Fig. 2A** shows that five genes (CDK6, SLC35D3, SLC25A27, PDGFD, and TRPC3) with decreased promoter methylation also have significant mRNA increase in G3K relative to MiaPaCa-2 cells. However, the other 5 genes have different outcomes (**Fig. 2B**). While the DUSP6 gene with decreased promoter methylation has reduced mRNA level, the OLIG1 and PTPRG genes with increased promoter methylation have increased mRNA levels in G3K relative to MiaPaCa-2 cells. The CDC42EP3 and ADORA2B genes with increased promoter methylation, interestingly, have no significant change in their

mRNA levels in G3K compared with MiaPaCa-2 cells. Hence, the change in methylation status in the promoter region does not necessarily associate with changes in expression.

Reversible demethylation and expression of PDGFD gene. To investigate the possible association of the altered expression of the above genes with acquired gemcitabine resistance, we determined protein product with a focus on TRPC3 and PDGFD, which have reduced promoter methylation and increased mRNA level in G3K cells. **Fig. 2C** shows that the TRPC3 protein level is similar between MiaPaCa-2 and G3K cells despite the difference in promoter methylation and mRNA level of TRPC3 in these cells. However, G3K cells produced much more PDGFD protein than MiaPaCa-2 cells (**Fig. 2D**). Thus, the expression of PDGFD gene with reduced promoter methylation in G3K cells is likely up-regulated at both mRNA and protein levels.

We next performed real-time RT-PCR and Western blot analyses to determine if the increased PDGFD production in G3K cells is indeed reversed in Rev cells as suggested from RRBS sequencing analysis. As shown in **Fig. 3A-B**, the increased PDGFD mRNA and protein levels in G3K cells diminished in Rev cells. To determine if the reversal in PDGFD expression is due to the change in PDGFD promoter methylation and to validate the RRBS data, we performed sodium-bisulfite sequencing analysis of 26 CpG dinucleotides residing in the promoter region of PDGFD gene in all three cell lines. For each cell line, four different clones were sequenced. As shown in **Fig. 3C**, 14-22 of the 26 CpG dinucleotides were methylated in MiaPaCa-2 cells. However, the same CpG dinucleotides were all demethylated in G3K cells. Interestingly, in Rev cells, 16-17 of these CpG dinucleotides were re-methylated. Thus, the PDGFD promoter is reversibly demethylated during acquisition of gemcitabine resistance, confirming the RRBS data and suggesting that the reversible demethylation may be responsible for the reversible increase of PDGFD expression in G3K cells.

PDGFD up-regulation contributes to gemcitabine resistance. To determine if the increased PDGFD expression in G3K cells potentially contributes to the acquired gemcitabine resistance, we first knocked down PDGFD in G3K cells followed by assay of cellular response to gemcitabine. **Fig. 3D** shows that PDGFD is efficiently knocked down by siRNA at both protein and mRNA levels, resulting in significant reduction of gemcitabine resistance (**Fig. 3E**). To eliminate the potential off-target issues of the PDGFD siRNA, we generated two stable clones from G3K cells (**Fig. 3F**) using two PDGFD shRNAs of different sequences and tested their response to gemcitabine compared with stable clones harboring scrambled shRNA. **Fig. 3G** shows that gemcitabine resistance is significantly reduced in both clones with PDGFD knockdown.

To further determine the role of PDGFD in gemcitabine resistance, stable clones (PD1 and PD2) over-expressing ectopic PDGFD were established from MiaPaCa-2 cells (**Fig. 3H)** and subjected to survival analysis against gemcitabine. **Fig. 3I** shows that these stable clones are 2-fold more resistant to gemcitabine than the control vector-transfected cells. Furthermore, MiaPaCa-2 cells cultured in G3K-conditioned media are also significantly more resistant to gemcitabine than cells cultured in regular media (**Fig. 3J**) and PDGFD knockdown in G3K cells significantly reduced conditioned-media-induced gemcitabine resistance (**Fig. 3K**). Thus, elevated PDGFD expression may contribute to the acquired gemcitabine resistance in G3K cells and the secreted PDGFD by the resistant cells may have paracrine effect on sensitive cells.

PDGFD up-regulation contributes to acquired gemcitabine resistance in Colo-357R cells. To eliminate potential cell line specificity of PDGFD effect on acquired gemcitabine resistance, we tested another PDAC cell line Colo-357R with acquired gemcitabine resistance compared with its parental Colo-357 cells (**Fig. 4A**) and found that Colo-357R cells also express higher levels of endogenous PDGFD mRNA (**Fig. 4B**) and protein (**Fig. 4C**) than Colo-357 cells. PDGFD

knockdown (**Fig. 4D**) significantly reduced gemcitabine resistance of Colo-357R cells (**Fig. 4E**) and PDGFD overexpression (**Fig. 4F**) increased gemcitabine resistance of Colo-357 cells (**Fig. 4G**). Thus, PDGFD up-regulation may be common in PDAC cells with acquired gemcitabine resistance and its relationship with gemcitabine resistance is unlikely specific to any cell line.

To further eliminate cell line specificity and to investigate the potential role of PDGFD in intrinsic gemcitabine resistance, we knocked down PDGFD in AsPC-1 cells (**Fig. 4H-I**) and tested its effect on cellular response to gemcitabine. As shown in **Fig. 4J**, PDGFD knockdown significantly reduced the intrinsic gemcitabine resistance of AsPC-1 cells. Thus, PDGFD expression likely contributes to both acquired and intrinsic gemcitabine resistance and confirmed its cell line-independent role in gemcitabine resistance.

STAT3 mediates PDGFD-induced gemcitabine resistance. PDGFD is known to activate several signaling pathways including PI3K/Akt and Notch (Wang et al., 2010). PDGFA and PDGFB are known to activate JAK/STAT3 pathway (Simeone-Penney, Severgnini, Rozo, Takahashi, Cochran & Simon, 2008; Vij, Sharma, Thakkar, Sinha & Mohan, 2008) although PDGFD has not been reported to do so. Because STAT3 is known to up-regulate in cancer cells with acquired resistance to erlotinib, vemurafenib, temozolomide, cisplatin, and paclitaxel (Duan et al., 2006; Huang et al., 2012; Lee, Ko, Joe, Kang & Hong, 2011; Li et al., 2013; Liu et al., 2013), we hypothesized that STAT3 might mediate PDGFD-induced gemcitabine resistance.

To test this hypothesis, we first examined STAT3 expression and activation in MiaPaCa-2 and G3K cells. As shown in **Fig. 5A**, both the Tyr^{705}-phosphorylated STAT3 (pSTAT3) and total STAT3 as well as STAT3 downstream targets VEGF and MMP2 were up-regulated in G3K compared with MiaPaCa-2 cells. More importantly, PDGFD knockdown in G3K cells led to reduction of pSTAT3, total STAT3, and its downstream targets (**Fig. 5B**). Similarly, PDGFD

knockdown in AsPC-1 cells also reduced the level of pSTAT3 and expression of its downstream target genes (data not shown). Consistently, over-expressing PDGFD in MiaPaCa-2 cells caused marked increase in the level of pSTAT3, total STAT3 and VEGF (**Fig. 5C**). Interestingly, in Rev cells pSTAT3 was reduced back to the basal level similar to that in MiaPaCa-2 cells, consistent with the reduced expression of STAT3 target gene VEGF (**Fig. 5D**) and with the reduced PDGFD expression (see above) in Rev cells although the total STAT3 level remained high (**Fig. 5D**), Thus, STAT3 may be a downstream effector of PDGFD up-regulation in G3K cells.

Next, we determined the potential role of STAT3 in gemcitabine resistance of G3K cells by knocking down STAT3. As shown in **Fig. 5E,** STAT3 knockdown significantly reduced gemcitabine resistance of G3K cells. Consistently, over-expressing a constitutively-activated STAT3 (Stat3c) in MiaPaCa-2 cells significantly increased gemcitabine resistance (**Fig. 5F**). Thus, STAT3 may be a downstream effector that mediates PDGFD-induced gemcitabine resistance.

PDGFD expression contributes to gemcitabine resistance of PDAC xenograft tumors and associates with poor clinical outcome in PDAC patients. To show that PDGFD over-expression contributes/causes gemcitabine resistance in vivo, we established xenograft tumors using the stable MiaPaCa-2 cells over-expressing PDGFD (PD1 clone) and vector-transfected control cells followed by gemcitabine treatment. As shown in **Fig. 6A-C**, both vector-transfected MiaPaCa-2 and PD1 xenograft tumors were eliminated by 120 mg/kg gemcitabine. However, at 60 mg/kg gemcitabine, the PD1 tumors continued to grow while the growth of the vector-transfected tumors was suppressed. Thus, the increased PDGFD expression likely contributes to in-vivo gemcitabine resistance. This conclusion is also corroborated by higher level of Ki67 and lower level of cleaved caspase 3 in the PD1 tumors compared with the vector-transfected tumors following 60 mg/kg gemcitabine treatment (**Fig. 6D**).

Finally, we determined if PDGFD expression potentially associates with clinical outcome of PDAC patients by taking advantage of the publicly available data. As shown in **Fig. 6E**, PDAC patients with high PDGFD expression had significant worse overall survival than patients with low PDGFD expression. This observation is consistent with our finding on the potential role of PDGFD in contribution to gemcitabine resistance.

DISCUSSION AND CONCLUSION

We showed here that the promoters of 65 genes had reversible methylation changes in the gemcitabine-selected G3K cells and that PDGFD expression was reversibly up-regulated due to reversible promoter demethylation. PDGFD up-regulation contributes to acquired gemcitabine resistance possibly via activating STAT3. Furthermore, PDGFD over-production by gemcitabine-resistant cells may confer bystander effect on gemcitabine sensitive cells via paracrine action.

Of the 65 genes that had reversible promoter methylation change, some had no change in their mRNA levels while others had increased mRNA level with increased methylation or decreased mRNA level with decreased methylation. These findings are peculiar since promoter methylations are usually thought to silence gene transcription. It is, however, possible that the promoter methylation in some cases may help recruit transcription factors to activate gene transcription (Gonzalez & Collier, 2013) while in other cases the transcription factors are insensitive to methylation status of promoter sequences (Tate & Bird, 1993). Furthermore, although the change in methylation resulted in change in mRNA level, it does not necessarily translate into changes in proteins (e.g., TRPC3). Thus, it is possible that only a fraction of the 65 genes with reversible methylation change in their promoter sequences has reversible alterations in the level of proteins.

It is also noteworthy that the 65 genes with reversible promoter methylation change do not represent all genes with reversible methylation. Firstly, the RRBS technology enriches reads on CGIs and, thus, has limited genomic coverage although this technology is accurate and results in single nucleotide resolution. Secondly, methylation silencing occurs in not only the promoter sequence, but also occurs in other regions. For example, the reversible CGI methylation of the 14-3-3σ gene occurs in the first exon (Qin, Dong & Zhang, 2014). Analysis of the 14-3-3σ gene methylation between MiaPaCa-2 and G3K cells revealed significant differential methylation ($p<9.23e-15$) although the read coverage is only 11.71% and only 4 of the 27 CpG dinucleotides were covered. Thus, filtration for the reversible promoter CGI methylations eliminated genes such as 14-3-3σ with reversible methylation change outside the promoter sequence.

In a previous study, we showed that the reversible methylation change of the 14-3-3σ gene in G3K cells is due to altered expression of DNMT1 and UHRF1 (Qin, Dong & Zhang, 2014). It is, thus, tempting to speculate that DNMT1 and UHRF1 may also be responsible for the reversible methylation change of the 65 genes including PDGFD. It, however, remains to be determined how the expression of DNMT1 and UHRF1 genes is changed during acquisition of gemcitabine resistance in G3K cells and during the partial loss of the resistance in Rev cells.

Identification of PDGFD as one of the genes with reversible methylation change and expression in the gemcitabine resistant G3K cells and its potential paracrine bystander effect are important findings for further understanding of drug resistance in cancer chemotherapy. PDGFD signaling is frequently deregulated in human malignancies including PDAC (Wang et al., 2007). The growing body of literature strongly suggests that PDGFD may be a key player in cancer development and progression by regulating several pathways such as PI3K/Akt, NF-κB, Notch, and MAPK pathways (Wang et al., 2010). In this study, we show that PDGFD also regulates

STAT3 pathway, which may mediate PDGFD-induced gemcitabine resistance. However, it is unknown if the other known PDGFD downstream effector pathways may also participate in the PDGFD-induced gemcitabine resistance.

Of the 65 genes with reversible methylation change, Wnt11 is another secretory factor that may be over-produced in G3K cells. Indeed, Wnt11 negatively associates with overall survival of PDAC patients, similar as PDGFD (unpublished observations). It is also noteworthy that, in addition to PDGFD, the methylation of PDGFB and PDGFC promoters was significantly reduced in G3K cells compared with MiaPaCa-2 cells although these demethylations were not reversed in Rev cells (see **Supplemental Table S2**). Considering that Rev cells are partially reversed in gemcitabine resistance (Qin, Dong & Zhang, 2014), the reduced methylation of PDGFB and PDGFC genes in G3K cells may result in higher expression level of these genes and contributes to the acquired gemcitabine resistance in G3K cells, but the lack of re-methylation of these genes in Rev cells possibly continue to contribute to the remaining resistance of Rev cells. Based on these findings, it is tempting to speculate that drug resistant cells may secrete factors that can activate various pathways to confer drug resistance for themselves and for the neighboring sensitive cells in the same micro-environment. This provocative concept deserves further testing.

ACKNOWLEDGEMENT

The authors wish to thank Dr. Keping Xie for the gift of Colo-357 and Colo-357R cells.

REFERENCES

Dong Z, Liu Z, Cui P, Pincheira R, Yang Y, Liu J*, et al.* (2009). Role of eIF3a in regulating cell cycle progression. Exp Cell Res 315**:** 1889-1894.

Duan Z, Foster R, Bell DA, Mahoney J, Wolak K, Vaidya A*, et al.* (2006). Signal transducers and activators of transcription 3 pathway activation in drug-resistant ovarian cancer. Clinical cancer research : an official journal of the American Association for Cancer Research 12**:** 5055-5063.

Gonzalez D, & Collier J (2013). DNA methylation by CcrM activates the transcription of two genes required for the division of Caulobacter crescentus. Mol Microbiol 88**:** 203-218.

Han B, Xie H, Chen Q, & Zhang JT (2006). Sensitizing hormone-refractory prostate cancer cells to drug treatment by targeting 14-3-3sigma. Mol Cancer Ther 5**:** 903-912.

Huang S, Chen M, Shen Y, Shen W, Guo H, Gao Q*, et al.* (2012). Inhibition of activated Stat3 reverses drug resistance to chemotherapeutic agents in gastric cancer cells. Cancer letters 315**:** 198-205.

Huang W, Dong Z, Chen Y, Wang F, Wang CJ, Peng H*, et al.* (2016). Small-molecule inhibitors targeting the DNA-binding domain of STAT3 suppress tumor growth, metastasis and STAT3 target gene expression in vivo. Oncogene 35**:** 783-792.

Lanczky A, Nagy A, Bottai G, Munkacsy G, Szabo A, Santarpia L*, et al.* (2016). miRpower: a web-tool to validate survival-associated miRNAs utilizing expression data from 2178 breast cancer patients. Breast Cancer Res Treat 160**:** 439-446.

Lee ES, Ko KK, Joe YA, Kang SG, & Hong YK (2011). Inhibition of STAT3 reverses drug resistance acquired in temozolomide-resistant human glioma cells. Oncology letters 2**:** 115-121.

Li R, Hu Z, Sun SY, Chen ZG, Owonikoko TK, Sica GL*, et al.* (2013). Niclosamide overcomes acquired resistance to erlotinib through suppression of STAT3 in non-small cell lung cancer. Molecular cancer therapeutics 12**:** 2200-2212.

Li R, Yu C, Li Y, Lam TW, Yiu SM, Kristiansen K*, et al.* (2009). SOAP2: an improved ultrafast tool for short read alignment. Bioinformatics 25**:** 1966-1967.

Li Y, Zhu J, Tian G, Li N, Li Q, Ye M*, et al.* (2010a). The DNA methylome of human peripheral blood mononuclear cells. PLoS biology 8**:** e1000533.

Li Z, Dong Z, Myer D, Yip-Schneider M, Liu J, Cui P*, et al.* (2010b). Role of 14-3-3sigma in poor prognosis and in radiation and drug resistance of human pancreatic cancers. BMC Cancer 10**:** 598.

Liu F, Cao J, Wu J, Sullivan K, Shen J, Ryu B*, et al.* (2013). Stat3-targeted therapies overcome the acquired resistance to vemurafenib in melanomas. The Journal of investigative dermatology 133**:** 2041-2049.

Liu Y, Liu H, Han B, & Zhang JT (2006). Identification of 14-3-3sigma as a contributor to drug resistance in human breast cancer cells using functional proteomic analysis. Cancer Res 66**:** 3248-3255.

Liu Z, Dong Z, Yang Z, Chen Q, Pan Y, Yang Y*, et al.* (2007). Role of eIF3a (eIF3 p170) in intestinal cell differentiation and its association with early development. Differentiation 75**:** 652-661.

Qi J, Dong Z, Liu J, Peery RC, Zhang S, Liu JY*, et al.* (2016). Effective Targeting of the Survivin Dimerization Interface with Small-Molecule Inhibitors. Cancer Res 76**:** 453-462.

Qin L, Dong Z, & Zhang JT (2014). Reversible epigenetic regulation of 14-3-3sigma expression in acquired gemcitabine resistance by uhrf1 and DNA methyltransferase 1. Mol Pharmacol 86**:** 561-569.

Qin L, Dong Z, & Zhang JT (2016). 14-3-3sigma regulation of and interaction with YAP1 in acquired gemcitabine resistance via promoting ribonucleotide reductase expression. Oncotarget (in press).

Simeone-Penney MC, Severgnini M, Rozo L, Takahashi S, Cochran BH, & Simon AR (2008). PDGF-induced human airway smooth muscle cell proliferation requires STAT3 and the small GTPase Rac1. Am J Physiol Lung Cell Mol Physiol 294**:** L698-704.

Tate PH, & Bird AP (1993). Effects of DNA methylation on DNA-binding proteins and gene expression. Curr Opin Genet Dev 3**:** 226-231.

Vij N, Sharma A, Thakkar M, Sinha S, & Mohan RR (2008). PDGF-driven proliferation, migration, and IL8 chemokine secretion in human corneal fibroblasts involve JAK2-STAT3 signaling pathway. Mol Vis 14**:** 1020-1027.

Voutsadakis IA (2011). Molecular predictors of gemcitabine response in pancreatic cancer. World J Gastrointest Oncol 3**:** 153-164.

Wang Z, Ahmad A, Li Y, Kong D, Azmi AS, Banerjee S*, et al.* (2010). Emerging roles of PDGF-D signaling pathway in tumor development and progression. Biochim Biophys Acta 1806**:** 122-130.

Wang Z, Kong D, Banerjee S, Li Y, Adsay NV, Abbruzzese J*, et al.* (2007). Down-regulation of platelet-derived growth factor-D inhibits cell growth and angiogenesis through inactivation of Notch-1 and nuclear factor-kappaB signaling. Cancer research 67**:** 11377-11385.

Yang Y, Chen Q, & Zhang JT (2002). Structural and functional consequences of mutating cysteine residues in the amino terminus of human multidrug resistance-associated protein 1. J Biol Chem 277**:** 44268-44277.

Yang Y, Liu Y, Dong Z, Xu J, Peng H, Liu Z*, et al.* (2007). Regulation of function by dimerization through the amino-terminal membrane-spanning domain of human ABCC1/MRP1. J Biol Chem 282**:** 8821-8830.

Table 1. Genes with reversible changes in promoter methylation

Genes with dcreased methylation in G3K and increased methylation in Rev Cells

Gene Symbol	DMR Fold Change (G3K/PaCa)	DMR Fold Change (Rev/G3K)
AFAP1L2	0.38	2.11
ANXA2P3	0.10	5.50
APBA1	0.42	2.14
CCNO	0.29	2.27
CDC42BPB	0.50	2.10
CDK6	0.22	2.62
CHRNA7	0.24	2.73
CRAMP1L	0.34	2.50
DDIT4L	0.29	5.56
DSE	0.24	3.00
DUSP6	0.28	3.39
EFNA5	0.05	∞^{b}
ELOVL2-AS1	0.35	2.92
FAM133B	0.28	3.30
FRAS1	0.29	2.38
FUOM	0.30	2.00
GALNT7	0.14	10.00
GNS	0.48	2.21
GRM4	0.43	2.67
H2AFY2	0.48	2.16
JMJD8	0.16	2.67
KIAA1324L	0.29	2.57
KIF21B	0.33	2.82
LOC100506190	0.44	2.05
LONRF3	0.47	2.03
MCTP1	0.49	2.29
MDFIC	0.03	15.00
MIR205HG	0.44	2.38
MMP25	0.15	4.67
MTA1	0.10	6.71
NKX1-2	0.46	2.18
PDGFD	0.16	5.88
PRDM1	0.12	3.75
RAET1G	0.31	4.00
RASD2	0.31	2.59
RNASET2	0.32	2.11
SEMA5B	0.50	2.25
SLC25A27	0.49	2.08
SLC31A2	0.46	2.30
SLC35D3	0.16	3.64
SOWAHD	0.47	2.17

TMEM181	0.40	2.50
TRPC3	0.25	2.35
WDR1	0.36	3.08
WNT11	0.21	2.67
ZNF593	0.27	2.63
ZNF669	0.10	18.50
ZNF808	0.38	5.75
ZNF83	0.26	4.00

Genes with increased methylation in G3K and decreased methylation in Rev Cells

Gene Symbol	DMR Fold Change (G3K/PaCa)	DMR Fold Change (Rev/G3K)
ADORA2B	2.00	0.48
CDC42EP3[c]	∞[b]	0.09
CDC42EP3[c]	29.00	1/∞[b]
CPNE7	4.25	0.44
FBXO27	7.75	0.45
JAG2	2.15	0.43
MIR1915	3.38	0.44
MRPS6	2.23	0.50
NPAS2	2.17	0.17
OLIG1	2.62	0.48
PTPRG	2.75	0.44
PWWP2B	2.79	0.49
SLC45A1	5.67	0.11
SNORD56B	3.29	0.06
SOX13	2.35	0.25
TNRC18	2.10	1/∞[a]
WNT9A	2.92	0.40

FIGURE LEGNEDS

Figure 1. RRBS sequencing results and genomic coverage. (A) Scheme in selection of G3K from MiaPaCa-2 cells and generation of G3KRev cells. (B) Comparison of RRBS sequencing results between MiaPaCa-2, G3K, and Rev cells. (C) Genomic coverage of promoter and CG island (CGI) numbers. (D) Genomic CpG coverage in promoter and CG island (CGI) at 4X and 10X depth. (E) Flowchart of differentially methylated region (DMR) filtration.

Figure 2. Characterization of candidate gene expression. (A-B) Real time RT-PCR analysis of mRNA levels of representative candidate genes with reversible methylation change changes in G3K cells (n=5, *p<0.05, **p<0.01, ***p<0.001). (C) Western blot analysis of TRPC3 protein in membrane fractions. MRP3 was used as a membrane protein loading control. (D) Western blot analysis of PDGFD in conditioned media. Commassie blue stained gel was used to show equal loading. The major band at 67-kDa in the commassie-stained gel may represent residual BSA derived from bovine serum in the prior culture media.

Figure 3. Reversible expression and gene demethylation of PDGFD in gemcitabine resistance. (A) Real-time RT-PCR analysis of PDGFD mRNA level. GAPDH was used as an internal control. (n=5, **p<0.01). (B) Western blot analysis of PDGFD in conditioned media. Commassie blue-stained gel was used to show equal loading. (C) Sodium bisulfite sequencing of PDGFD promoter CGI. Four clones from each cell line were isolated for sequencing. Solid and open circles represent methylated and unmethylated cytosines, respectively. The chromatograms are sequence profiles containing CpG dinucleotides 1-12 for MiaPaCa-2, G3K, and Rev cells. The underlined nucleotides are cytosines that are demethylated in G3K cells. (D, F, H) Western blot or real-time RT-PCR analysis of PDGFD expression in G3K cells with transient (D) or stable (F) PDGFD knockdown and in MiaPaCa-2 cells with stable PDGFD over-expression (H). Commassie

blue-stained gel was used to show equal loading (H). (E, G, I), Effect of PDGFD knockdown (E, G) or over-expression (I) on gemcitabine resistance as determined using survival assays as described in Materials and Methods. (J and K) Effect of conditioned media from G3K cells without (J) or with PDGFD knockdown (K) on gemcitabine response of MiaPaCa-2 cells. RRF=relative resistance factor. (n=5, *p<0.05, **p<0.01, ***p<0.001). RM=regular media; CM=G3K-conditioned media.

Figure 4. Role of PDGFD in acquired and intrinsic gemcitabine resistance. (A-B) Real-time RT-PCR (A) and Western blot (B) analyses of endogenous PDGFD in parental Colo-357 and gemcitabine resistant Colo-357R cells. (C) Relative resistance to gemcitabine of the parental Colo-357 and Colo-357R cells. (D, F, H, I) Real-time RT-PCR or Western blot analysis of PDGFD expression following PDGFD knockdown (D, H, I) or ectopic over-expression (F) in Colo-357, Colo-357R, or AsPC1 cells. (E, G, J) Effect of PDGFD knockdown (E, J) or over-expression (G) on gemcitabine resistance. (n=5-6, *p<0.05, **p<0.01, ***p<0.001).

Figure 5. PDGFD regulation of STAT3 signaling and its role in gemcitabine resistance. (A) Western blot analysis of total STAT3, pSTAT3, secreted PDGFD, VEGF, and MMP2 in MiaPaca-2 and G3K cells. (B-C) Effect of PDGFD knockdown (B) and over-expression (C) on STAT3 signaling in G3K and MiaPaCa-2 cells, respectively, as determined using Western blot analysis. (D) Western blot analysis of STAT3 signaling in MiaPaCa-2, G3K, and Rev cells. (E-F) Effect of STAT3 knockdown (E) or STAT3c over-expression (F) on gemcitabine resistance. (n=5, **p<0.01). Actin was used as a loading control.

Figure 6. PDGFD in in-vivo gemcitabine resistance and association with PDAC patient outcome. (A) Gemcitabine effect on growth of xenograft tumors derived from MiaPaCa-2 cells transfected with vector (Vec) or over-expressing PDGFD (PD1 clone) and body weight of

mice carrying xenograft tumors. (B, C) Gross anatomy (B) and wet weight of xenograft tumors at the end of treatments. (D) Immunohistochemistry staining of PDGFD, Ki67, and cleaved caspase 3 in xenograft tumors of different treatment groups. (E) Association of PDGFD expression with overall survival of PDAC patients with 60 months cutoff.

Figure 1

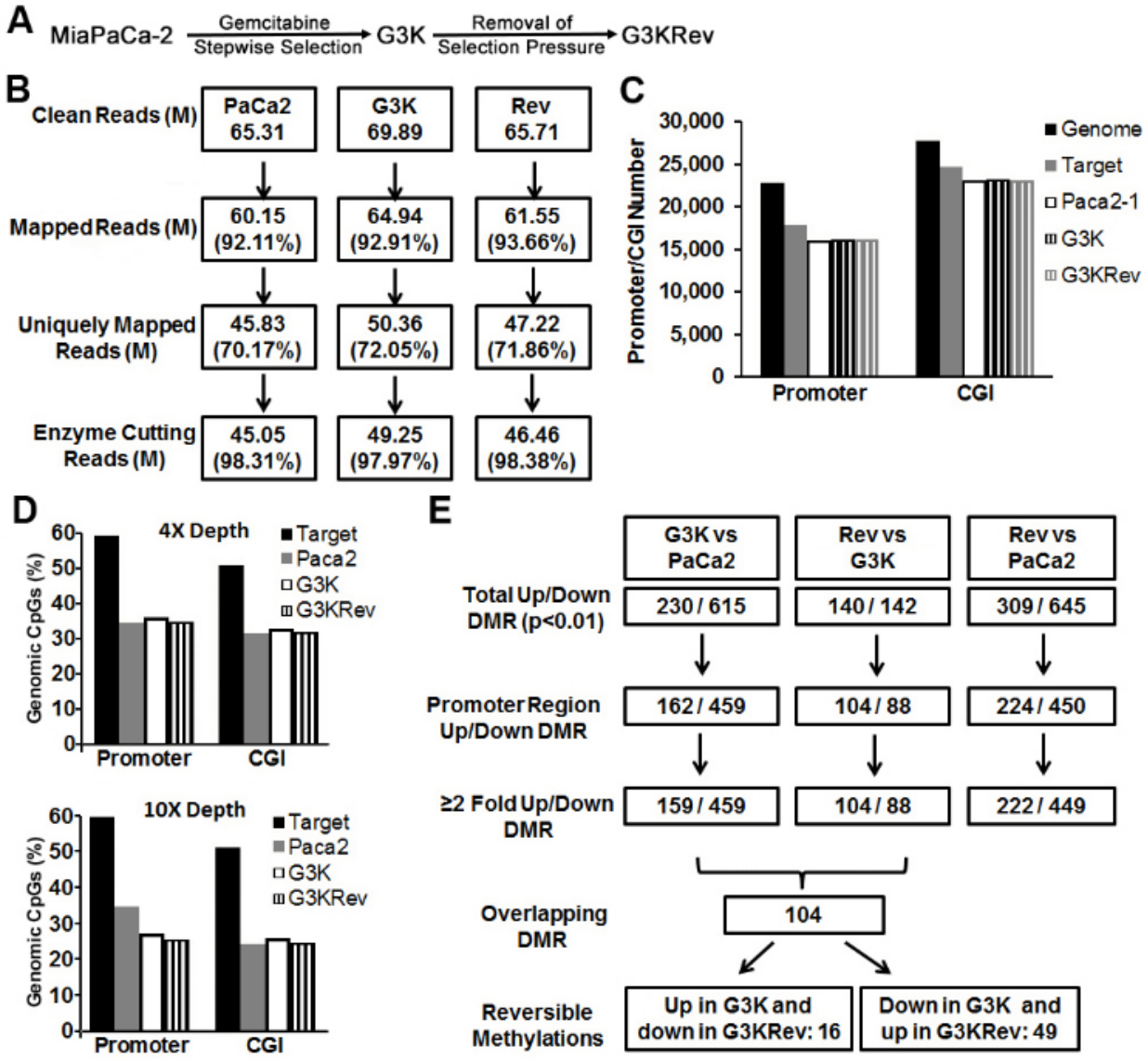
A
MiaPaCa-2
Gemcitabine Stepwise Selection
G3K
Removal of Selection Pressure
G3KRev
B
Clean Reads (M)
PaCa2 65.31
G3K 69.89
Rev 65.71
Mapped Reads (M)
60.15 (92.11%)
64.94 (92.91%)
61.55 (93.66%)
Uniquely Mapped Reads (M)
45.83 (70.17%)
50.36 (72.05%)
47.22 (71.86%)
Enzyme Cutting Reads (M)
45.05 (98.31%)
49.25 (97.97%)
46.46 (98.38%)
C
Promoter/CGI Number
30,000
25,000
20,000
15,000
10,000
5,000
0
Genome
Target
Paca2-1
G3K
G3KRev
Promoter
CGI
D
4X Depth
Target
Paca2
G3K
G3KRev
Genomic CpGs (%)
60
50
40
30
20
10
0
Promoter
CGI
10X Depth
Target
Paca2
G3K
G3KRev
Genomic CpGs (%)
60
50
40
30
20
10
0
Promoter
CGI
E
G3K vs PaCa2
Rev vs G3K
Rev vs PaCa2
Total Up/Down DMR (p<0.01)
230 / 615
140 / 142
309 / 645
Promoter Region Up/Down DMR
162 / 459
104 / 88
224 / 450
≥2 Fold Up/Down DMR
159 / 459
104 / 88
222 / 449
Overlapping DMR
104
Reversible Methylations
Up in G3K and down in G3KRev: 16
Down in G3K and up in G3KRev: 49

Figure 2

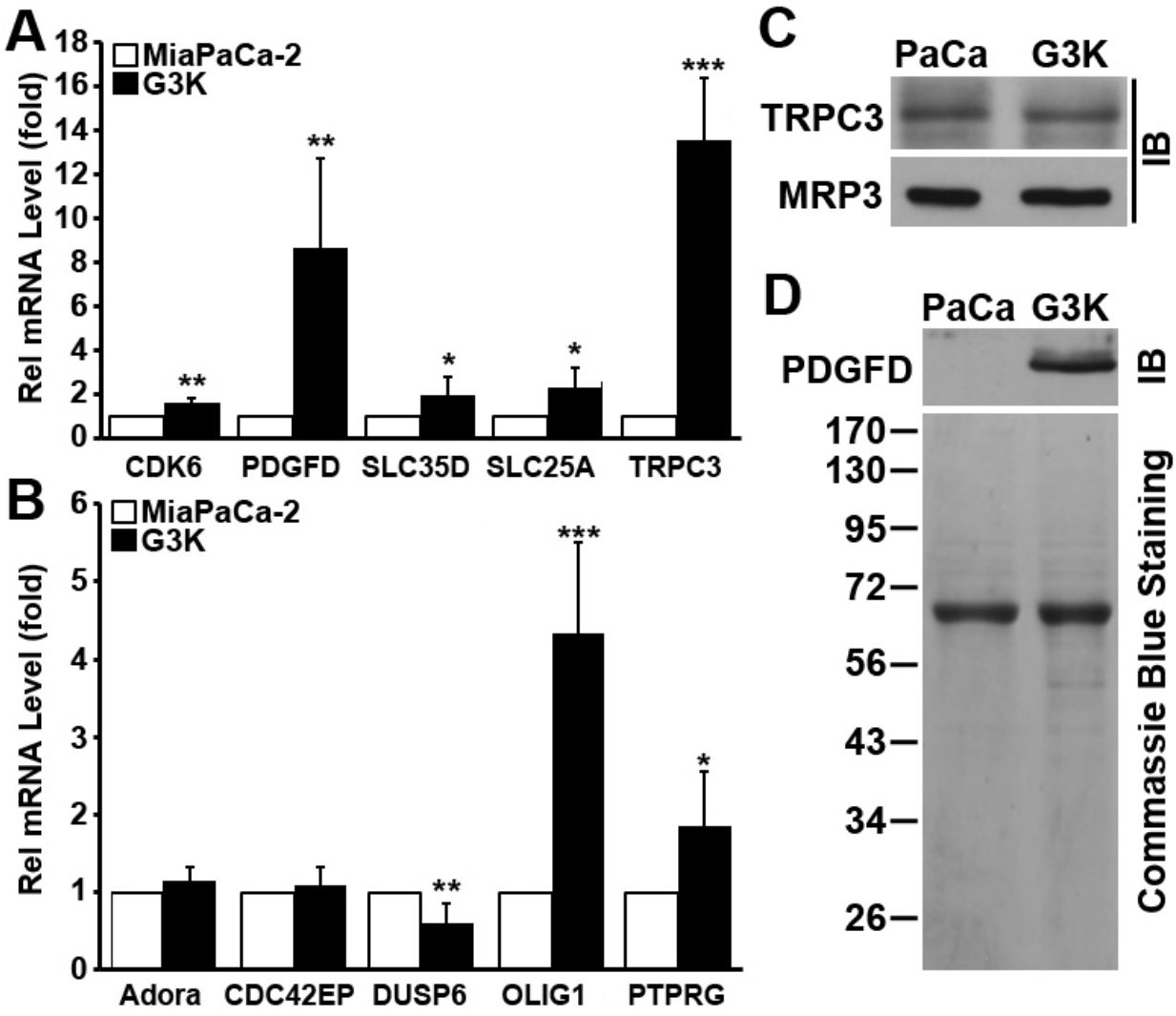
A
MiaPaCa-2
G3K
Rel mRNA Level (fold)
CDK6
PDGFD
SLC35D
SLC25A
TRPC3
B
MiaPaCa-2
G3K
Rel mRNA Level (fold)
Adora
CDC42EP
DUSP6
OLIG1
PTPRG
C
PaCa
G3K
TRPC3
MRP3
IB
D
PaCa
G3K
PDGFD
IB
170
130
95
72
56
43
34
26
Commassie Blue Staining

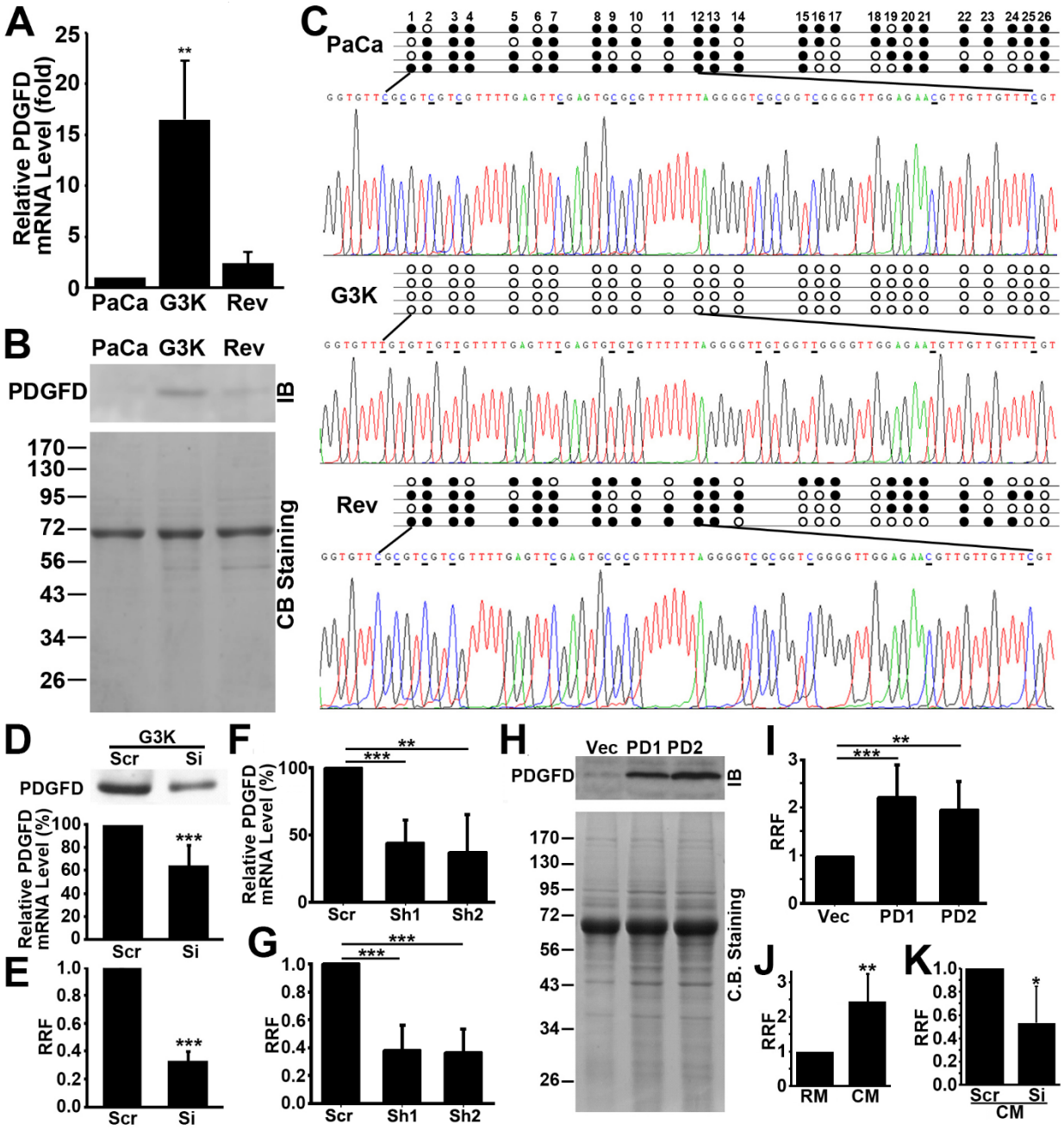
A
Relative PDGFD mRNA Level (fold)
PaCa G3K Rev
B
PaCa G3K Rev
PDGFD
IB
CB Staining
C
PaCa
G3K
Rev
D
G3K
Scr Si
PDGFD
Relative PDGFD mRNA Level (%)
E
RRF
F
Relative PDGFD mRNA Level (%)
Scr Sh1 Sh2
G
RRF
H
Vec PD1 PD2
PDGFD
IB
C.B. Staining
I
RRF
Vec PD1 PD2
J
RRF
RM CM
K
RRF
Scr Si
CM

Figure 4

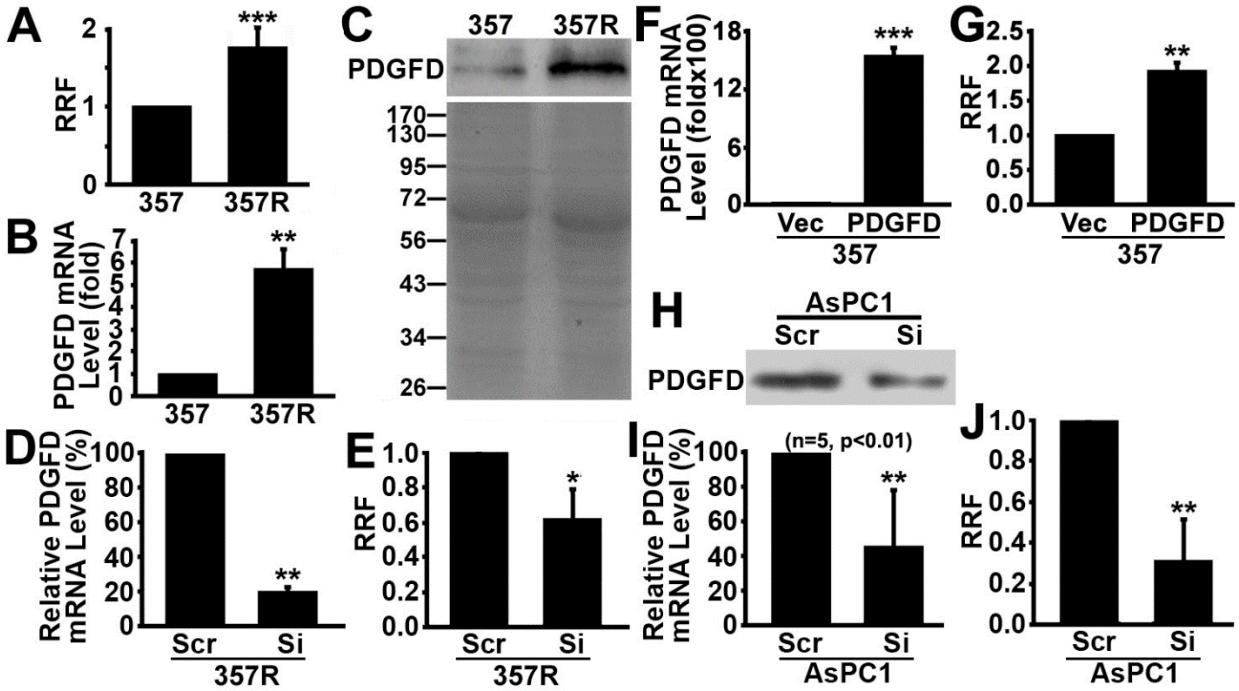
A
RRF
357
357R
B
PDGFD mRNA Level (fold)
C
357
357R
PDGFD
170
130
95
72
56
43
34
26
F
PDGFD mRNA Level (foldx100)
Vec
PDGFD
357
G
RRF
H
AsPC1
Scr
Si
PDGFD
D
Relative PDGFD mRNA Level (%)
E
I
(n=5, p<0.01)
J

Figure 5

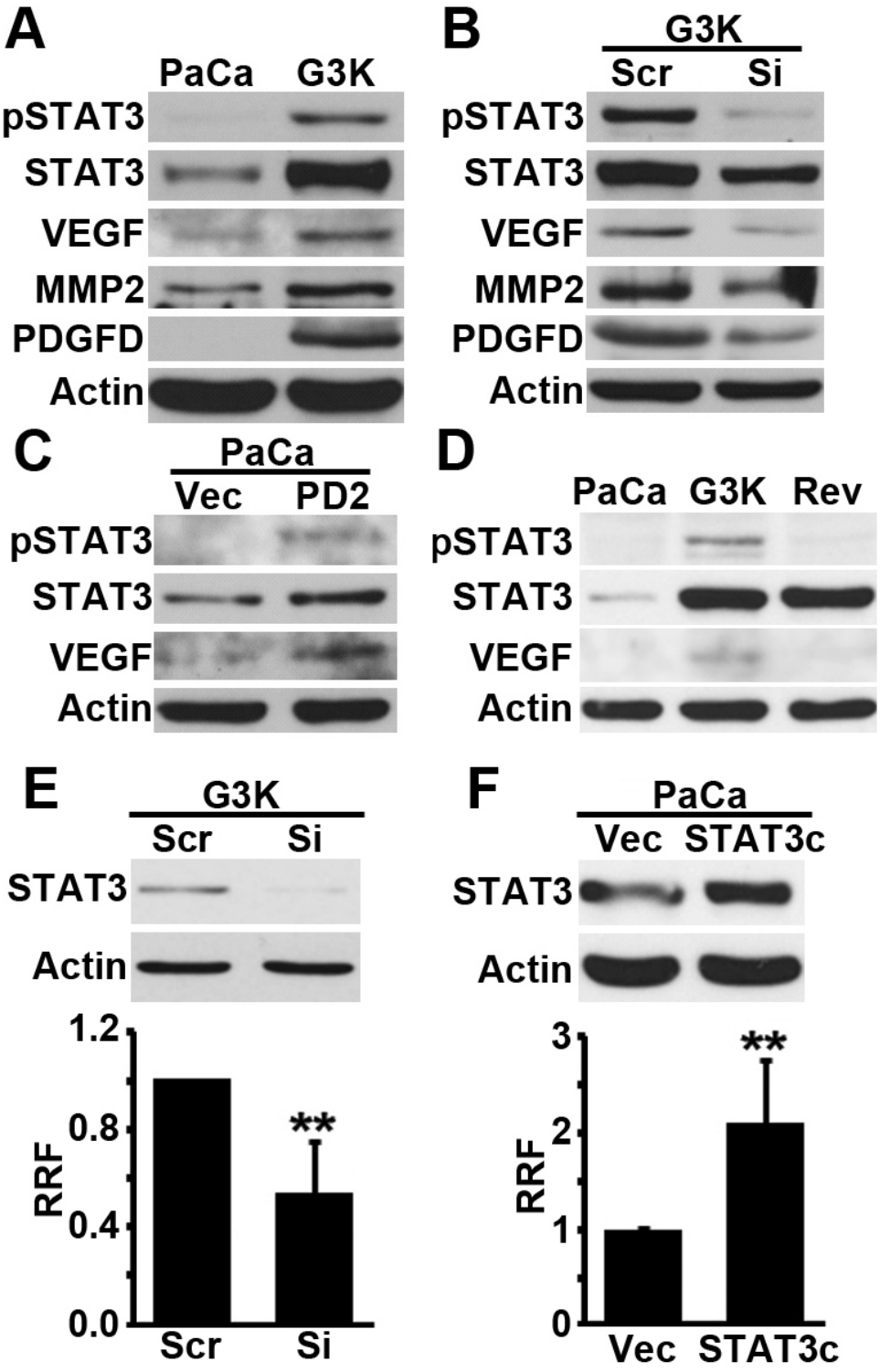
A
PaCa
G3K
pSTAT3
STAT3
VEGF
MMP2
PDGFD
Actin
B
G3K
Scr
Si
pSTAT3
STAT3
VEGF
MMP2
PDGFD
Actin
C
PaCa
Vec
PD2
pSTAT3
STAT3
VEGF
Actin
D
PaCa
G3K
Rev
pSTAT3
STAT3
VEGF
Actin
E
G3K
Scr
Si
STAT3
Actin
RRF
1.2
0.8
0.4
0.0
**
Scr
Si
F
PaCa
Vec
STAT3c
STAT3
Actin
RRF
3
2
1
0
**
Vec
STAT3c

Figure 6

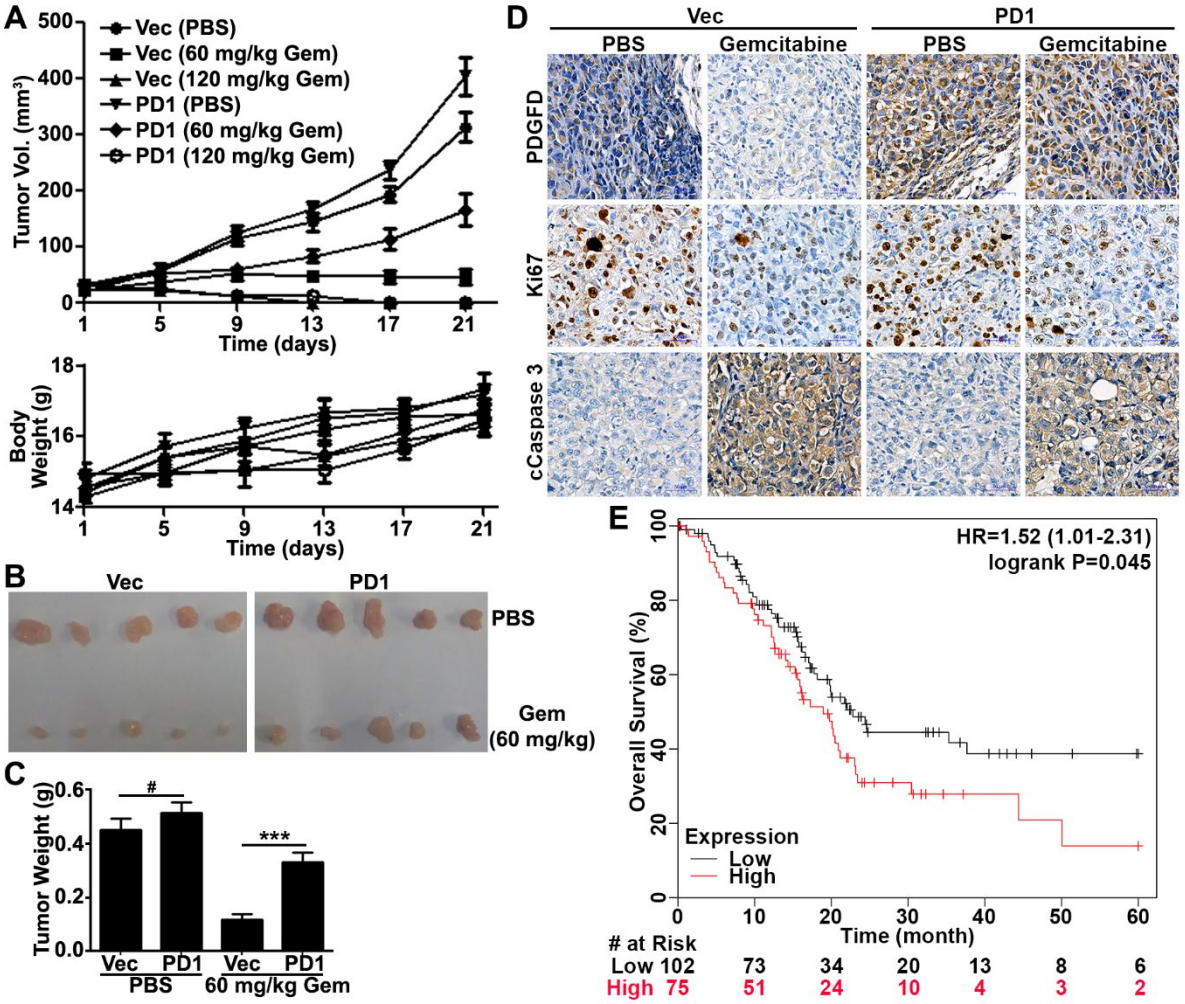
A
Vec (PBS)
Vec (60 mg/kg Gem)
Vec (120 mg/kg Gem)
PD1 (PBS)
PD1 (60 mg/kg Gem)
PD1 (120 mg/kg Gem)
Tumor Vol. (mm³)
Time (days)
Body Weight (g)
Time (days)
B
Vec
PD1
PBS
Gem (60 mg/kg)
C
Tumor Weight (g)
#
***
Vec PD1 Vec PD1
PBS
60 mg/kg Gem
D
Vec
PD1
PBS
Gemcitabine
PBS
Gemcitabine
PDGFD
Ki67
cCaspase 3
E
HR=1.52 (1.01-2.31)
logrank P=0.045
Overall Survival (%)
Expression
Low
High
Time (month)
at Risk
Low 102 73 34 20 13 8 6
High 75 51 24 10 4 3 2